NSWC/DL TR-3530

SHOCK WAVE COMPRESSION OF AN ALUMINA-FILLED EPOXY

by
W. MOCK, Jr.
W. H. HOLT
Armaments Development Department

DECEMBER 1976

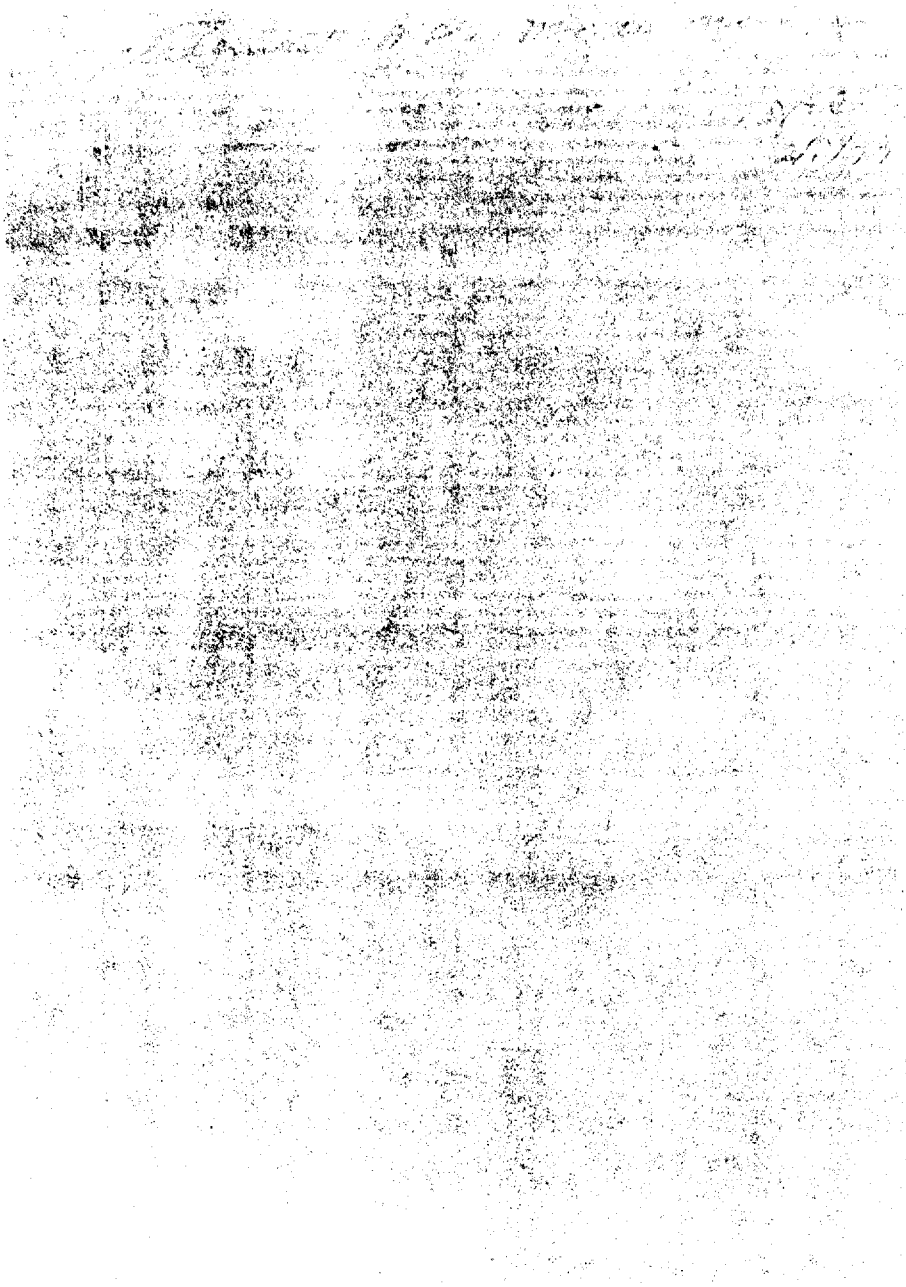

UNCLASSIFIED

SECURITY CLASSIFICATION OF THIS PAGE (When Data Entered)

REPORT DOCUMENTATION PAGE

READ INSTRUCTIONS BEFORE COMPLETING FORM

1. REPORT NUMBER: TR-3530

2. GOVT ACCESSION NO.: NSWC/DL-TR-3530

3. RECIPIENT'S CATALOG NUMBER:

4. TITLE (and Subtitle): SHOCK WAVE COMPRESSION OF AN ALUMINA-FILLED EPOXY

5. TYPE OF REPORT & PERIOD COVERED: Final rept.

6. PERFORMING ORG. REPORT NUMBER:

7. AUTHOR(s): W. Mock, Jr.
W. H. Holt

8. CONTRACT OR GRANT NUMBER(s): 15p.

9. PERFORMING ORGANIZATION NAME AND ADDRESS
Naval Surface Weapons Center (DG-50)
Dahlgren Laboratory
Dahlgren, Virginia 22448

10. PROGRAM ELEMENT, PROJECT, TASK AREA & WORK UNIT NUMBERS:

11. CONTROLLING OFFICE NAME AND ADDRESS:

12. REPORT DATE: December 1976

13. NUMBER OF PAGES: 19

14. MONITORING AGENCY NAME & ADDRESS (if different from Controlling Office):

15. SECURITY CLASS. (of this report): UNCLASSIFIED

15a. DECLASSIFICATION/DOWNGRADING SCHEDULE:

16. DISTRIBUTION STATEMENT (of this Report)

Approved for public release; distribution unlimited.

17. DISTRIBUTION STATEMENT (of the abstract entered in Block 20, if different from Report)

18. SUPPLEMENTARY NOTES

19. KEY WORDS (Continue on reverse side if necessary and identify by block number)
Wave Propagation
Alumina-filled Epoxy
Shock Wave Equation of State
Gas Gun

20. ABSTRACT (Continue on reverse side if necessary and identify by block number)

The shock wave equation of state for an alumina-filled epoxy, Castall 300, has been determined in the stress range from 0.4 to 3.7 GPa via gas gun experiments. Stress - particle velocity data was obtained by impacting Castall disks directly onto quartz gauges. Shock transit-time experiments were performed by impacting epoxy specimens surrounded by tilt pins and backed with quartz gauges. The results are compared with the shock response of an unfilled epoxy resin and an alumina-filled epoxy of different density.

DD FORM 1473 EDITION OF 1 NOV 65 IS OBSOLETE

S/N 0102-LF-014-6601

UNCLASSIFIED

SECURITY CLASSIFICATION OF THIS PAGE (When Data Entered)

FOREWORD

The shock wave properties of an alumina-filled epoxy material have been measured in the low gigapascal stress range. These properties are important for applications involving the combined environments of high voltage and shock stress. Funding for this work was provided by NAVAIR Task No. A350-3500/004C/6WTW27-001.

This report has been reviewed by C. A. Cooper, Head, Munitions Division.

Released by:

CDR JAMES R. WILLIAMS
Acting Assistant Head
Military Applications
Armaments Development Department

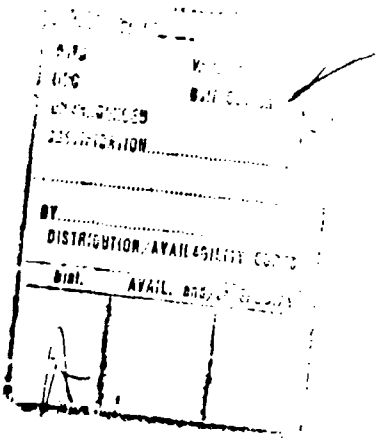

TABLE OF CONTENTS

LIST OF ILLUSTRATIONS

LIST OF TABLES

INTRODUCTION

Alumina-filled epoxy composites are used in high-voltage applications because of their high dielectric strengths. One application is the encapsulation of ferroelectric elements for shock depoling.[1] Only a few investigations have been reported on the shock response of these composite materials.[2,3] This report describes the measurement of the shock wave equation of state for a commercially available alumina-filled epoxy, Castall 300 resin and RT 7 hardener,[4] in the stress range from approximately 0.4 to 3.7 GPa.

Castall 300 - RT 7 epoxy contains five constituents with the following weight percentages: 66.7% Al_2O_3 particles, 21.8% Castall 100 unfilled epoxy, 7.4% RT 7 hardener, 2.7% lamp black, and 1.4% of an additional proprietary ingredient. The volume fraction of Al_2O_3 particles for this mixture is 0.37. The particles vary in size between 2 and 50 μm with the median size being 8 μm.[5]

In addition to the shock wave measurements, the zero-pressure ultrasonic longitudinal wave velocity was measured for comparison with the zero-particle-velocity intercept of the shock velocity - particle velocity data. The experimental techniques used for the shock wave and ultrasonic measurements are presented in the next section. Results are discussed in the third section.

EXPERIMENTAL TECHNIQUES

The shock wave measurements were performed with a gas gun.[6] A schematic of the gun is shown in Figure 1. The bore diameter is 40 mm. A projectile with impactor disk is loaded into the barrel and a target assembly containing the specimen is mounted on the muzzle. The barrel is evacuated to 0.1 Pa pressure to minimize gas cushion effects at impact.

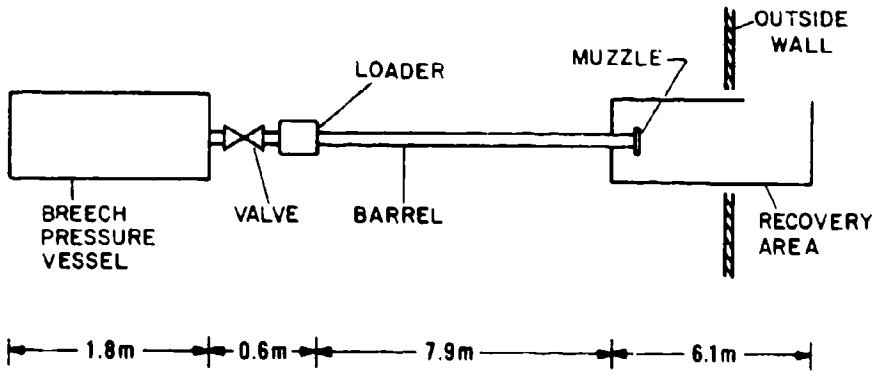

Figure 1. Schematic of Gas Gun

The gun is fired by actuating the fast opening valve. The projectile impact velocity can be varied in a controlled manner over the range from 0.03 to 1 km/s.

A series of experiments was performed in which a Castall disk was impacted onto a quartz gauge. In this type of experiment the Castall shock stress σ and particle velocity u are measured. The Castall impactor and quartz gauge are stressed directly in uniaxial compression. The shock stress σ is calculated from the measured quartz gauge current i_q. This is done by using the relationship between i_q and the shock stress σ_q in the quartz gauge[7] and the equation $\sigma = \sigma_q$. The particle velocity u can be obtained from the mass continuity equation across the impact interface:

$$u = U_o - u_q \tag{1}$$

where U_o is the measured projectile velocity and u_q is the quartz particle velocity calculated from σ_q using the constitutive equation for quartz. The Castall shock velocity U is obtained from the Hugoniot shock wave equation

$$\sigma = \rho_o U u \qquad (2)$$

where ρ_o is the initial Castall density.

Shunted guard-ring quartz gauges were used in these experiments (Valpey-Fisher No. VC-B-11-01-0006). The read time for these gauges is approximately 230 ns; this is the time required for the shock stress to propagate through the thickness of the quartz disk.

A series of shock transit-time experiments was performed on Castall disks to measure the shock velocity, the particle velocity, and the time dependence of the stress. Figure 2 is a schematic of the muzzle region for these measurements. Either a quartz or Castall disk is impacted onto the specimen. The average projectile velocity at impact is measured with the three charged pins in the side of the barrel. The impact time is measured by the four tilt pins which are placed around the specimen. The

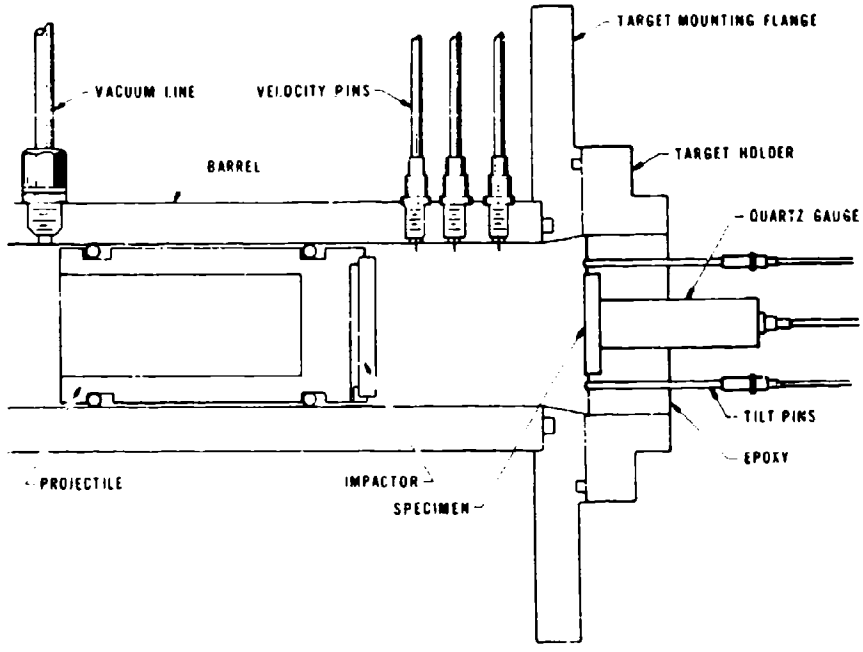

Figure 2. Schematic of Muzzle Region for Shock Transit-Time Measurement

tilt pin ends are positioned in the plane of the impact face of the specimen to within 1 μm. A quartz gauge or piezoelectric pin (Valpey-Fisher Pinduc No. VP-1093-1.5) is centered on the back of the specimen to measure the time when the stress wave reaches it. The quartz gauge measures the stress-time profile at the specimen-quartz interface and the pinducer indicates the arrival of the stress wave at the interface. The shock transit time is determined by measuring the time difference between the tilt data and the quartz gauge or pinducer data. A Berkley Nucleonics digital delay generator with 1-ns resolution is used for producing two reference pulses which are time delayed with respect to each other by a predetermined amount. The initial pulse is recorded on the tilt data trace and the delayed pulse is recorded on the quartz gauge or pinducer data trace. A toolmaker's microscope is used to obtain pulse amplitude and time information from the data traces.

The ultrasonic pulse-echo technique was used for the longitudinal wave velocity measurements on Castall disks for comparison with the zero-particle-velocity intercept data. A Panametrics Pulser-Receiver and Dapco transducers were used for the measurements. The time difference between the echos was measured using a Tektronix oscilloscope with a digital delay plug-in having 1-ns resolution.

RESULTS AND DISCUSSION

The average measured density for the Castall disks is 2.21 Mg/m^3. A summary of the shock wave data is given in Table 1. A brief description of a shot is given in the second column of the table. Impact tilt was measured in three transit-time experiments with the tilt pin technique, and was obtained from the risetime of the quartz gauge pulse in the direct-impact experiments. The average tilt value for the shots is 2.6 mrad. The projectile velocity accuracy is 0.2%. The estimated particle velocity accuracy is 1%; the shock stress and shock velocity accuracy is estimated to be 2-3%.

Table 1. Shock Wave Data for Castall 300 - RT 7 Epoxy

Shot No.	Description	Projectile Velocity km/s	Specimen Thickness mm	Particle Velocity km/s	Shock Velocity km/s	Stress GPa	$\frac{\Delta V}{V_o}$
125	Castall → Castall/tilt pins, quartz gauge	0.102	6.370	0.051	3.13	0.353	0.0162
130	Castall → quartz gauge	0.119	3.79	0.086	2.66	0.505	0.0322
62	Castall → quartz gauge	0.149	3.188	0.105	2.86	0.665	0.0367
131	Castall → Castall/tilt pins, quartz gauge	0.352	6.387	0.176	3.04	1.18	0.0580
64	Castall → quartz gauge	0.275	3.193	0.189	3.11	1.31	0.0608
126	Castall → quartz gauge	0.390	2.79	0.265	3.26	1.91	0.0814
65	Castall → Castall/tilt pins, pinducer	0.566	6.380	0.293	3.29	2.05	0.0859
67	Quartz → Castall/tilt pins, pinducer	0.557	6.393	0.373	3.45	2.83	0.106
127	Castall → quartz gauge	0.721	2.79	0.479	3.59	3.72	0.137

Previous work on the viscoelastic materials Epon 828 epoxy[8] and polymethyl methacrylate[9] (PMMA) indicate that shock waves in these materials are nonsteady and dispersive under some conditions but that for sufficient sample thicknesses and shock stress amplitudes the waves become steady. Similar phenomena is expected in Castall 300 which is a viscoelastic composite material. Steady waves are achieved for Epon 828 for a particle velocity and sample thickness greater than 0.1 km/s and 9.5 mm, respectively.[8] In order to apply the Hugoniot equilibrium equations to the transit-time experiments it is assumed that the waves are steady. Based on the Epon 828 criteria this may not be strictly true for the shot with the lowest particle velocity.

For the two transit-time measurements with back-surface quartz gauges, the shock velocity was determined from the half-amplitude value of the quartz gauge pulse. This velocity can be used with the Hugoniot equations to give the equilibrium response of the material.[8] For the back-surface measurements the signal was sufficiently spread out in time due to the

dispersive nature of Castall that the entire signal was not recorded during the read time of the gauge. The signals reached about 70% of their estimated maximum value based on an incident shock stress calculated from the direct-impact experiments. An estimated error of only about 2% in the shock velocity measurements was introduced by using the actual (compared to the expected) half-amplitude values because the shock transit times were sufficiently long (~2 μs) compared to the half-amplitude uncertainty.

Two measurements of the shock transit time were made with back-surface pinducers. The velocities for these measurements may be a few percent too large since a pinducer measurement yields the first-signal velocity, albeit a straight-line least-squares fit of the shock velocity - particle velocity data was not appreciably affected by deleting these shots.

The last column in Table 1 gives the unaxial strain ε for the Castall system. The strain is given by

$$\varepsilon = \frac{u}{U} = \frac{V_o - V}{V_o} = \frac{\Delta V}{V_o} \qquad (3)$$

where $V_o = \rho_o^{-1}$ and $V = \rho^{-1}$ are the initial and final specific volumes, respectively, for the material.

A quartz gauge record from a direct-impact experiment is shown in Figure 3. The read time for the gauge is the duration of the first positive current pulse. The stress in the Castall impactor is obtained from the initial jump in the current. Figure 4 is a quartz gauge pulse from a back-surface measurement. The risetime of this pulse is large compared with that for the direct-impact experiment (Figure 3) due to the dispersive nature of this composite material.

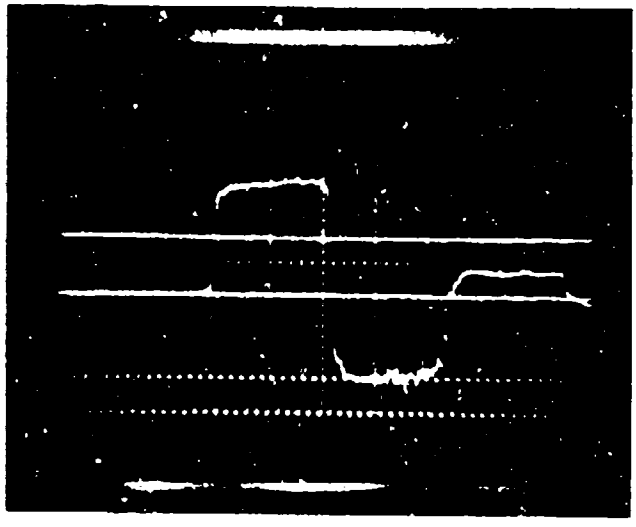

Figure 3. Quartz Gauge Pulse From Direct-Impact Experiment (Time increases from left to right. The current calibration trace (upper horizontal line) has an amplitude of 120 mA. The quartz-gauge current amplitude is 221 mA corresponding to a stress of 1.9 GPa. A 20-ns-period time calibration wave is shown at the bottom.)

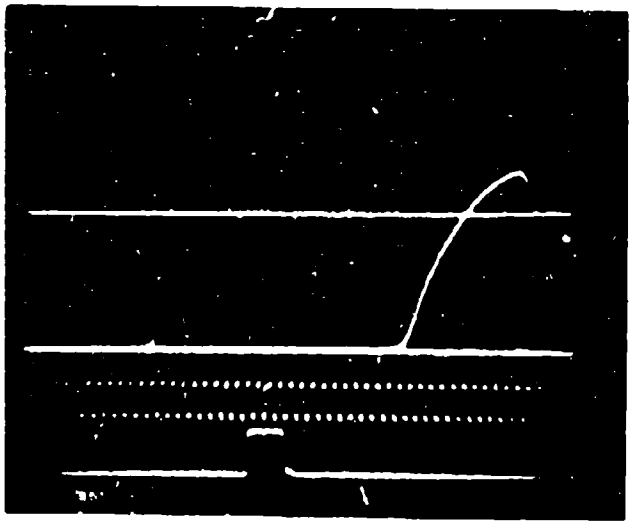

Figure 4. Quartz Gauge Pulse From Transmitted-Wave Experiment (Time increases from left to right. The current calibration trace (upper horizontal line) has an amplitude of 100 mA. A 20-ns-period time calibration wave is the middle trace. The time-reference square pulse at the bottom is used for measuring the wave velocity in the specimen.)

A plot of the Castall shock velocity - particle velocity (U, u) data is given in Figure 5. The scatter in the U, u point with the lowest particle velocity may be due to impact tilt or wave nonsteadiness. A straight-line least-squares fit of the data gives U = 2.78 + 1.63 u for the shock wave equation of state in the stress range 0.4 to 3.7 GPa. The average value for the ultrasonic longitudinal wave velocity is 2.88 km/s for a 2 to 4 MHz center frequency of a broad-band pulse. This value is only about 4% larger than the zero-particle-velocity intercept of 2.78 km/s obtained from the shock data, indicating that the ultrasonic and U, u intercept velocities are in agreement. The equation of state for a different alumina-filled epoxy with a larger density and volume fraction of Al_2O_3 particles[3] than Castall is shown for comparison. The U, u curve for unfilled Epon 828-Z[8] is also shown. Comparison of the curves for these materials in this stress range indicates that the addition of Al_2O_3 particles to an unfilled epoxy shifts the curve upward with minimum

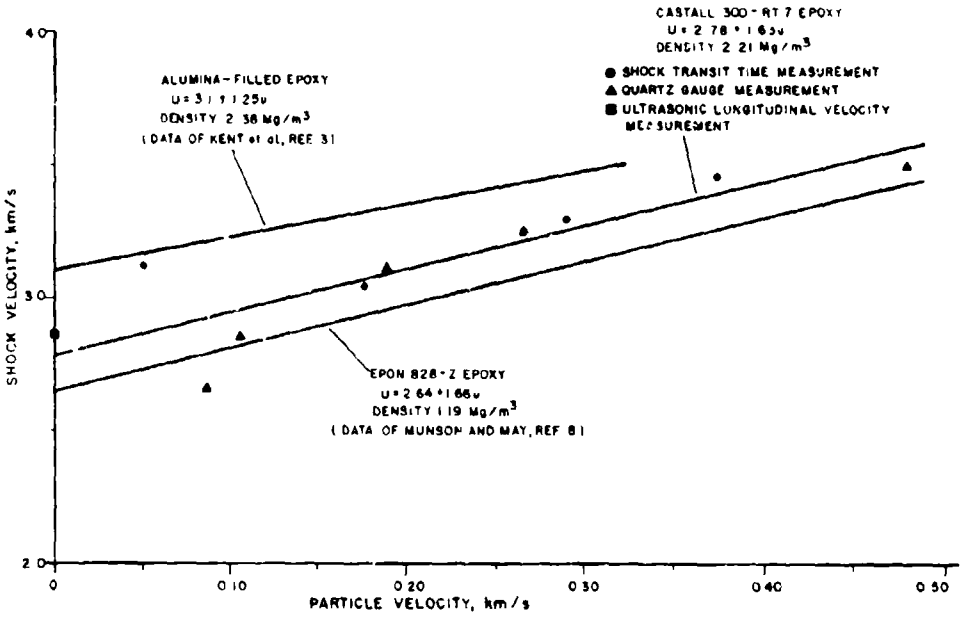

Figure 5. Shock Velocity - Particle Velocity Relationship for Castall 300 - RT 7 Epoxy

slope change. These results also show that the epoxy matrix still controls the U, u dependance for the composite, since even with a large addition (~40 volume %) of higher wave velocity (~8 km/s) particles the shock velocity of the composite increases only on the order of 10%.

Figure 6 shows the data points and the resulting stress - particle velocity relationship for Castall determined from the U, u relation and Equation 2. The curves for the higher density alumina-filled epoxy and the unfilled Epon 828-Z epoxy are shown for comparison.

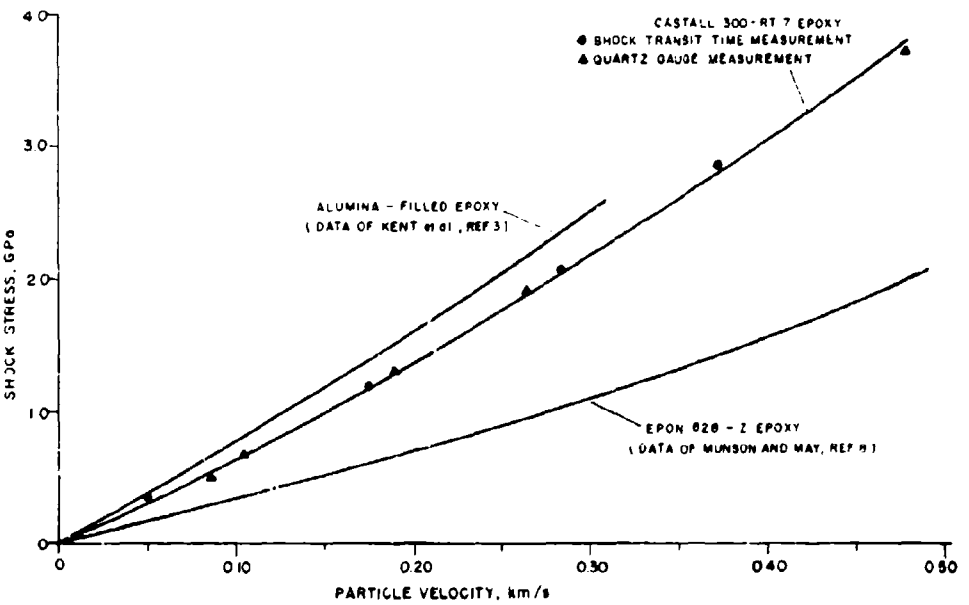

Figure 6. Stress - Particle Velocity Relationship for Castall 300 - RT 7 Epoxy

SUMMARY

The shock wave equation of state for Castall 300 alumina-filled epoxy has been determined in the stress range from 0.4 to 3.7 GPa with a gas gun. The results are compared with the equation of state for an unfilled epoxy resin and an alumina-filled epoxy of different density.

REFERENCES

1. P. C. Lysne and C. M. Percival, "Electric Energy Generation by Shock Compression of Ferroelectric Ceramics: Normal Mode Response of PZT 95/5," Journal of Applied Physics, Vol. 46, p. 1519 (1975).

2. D. E. Munson and K. W. Schuler, "Hugoniot Predictions for Mechanical Mixtures Using Effective Moduli," Shock Waves and the Mechanical Properties of Solids, edited by J. J. Burke and V. Weiss, Syracuse University Press, Syracuse, New York, p. 185 (1971).

3. L. Kent, K. J. Bowen and B. M. Butcher, "The Performance of Manganin Wire Gages in Aluminum Oxide Filled Epoxy," Sandia Laboratories Report SC-DR-70-291, Albuquerque, New Mexico (June 1970).

4. Castall, Inc., East Weymouth, Massachusetts, 02189.

5. Technical information for the Castall 300 - RT 7 epoxy was furnished by Mr. Al Alekna of Castall, Inc.

6. W. Mock, Jr. and W. H. Holt, "The NSWC Gas Gun Facility for Shock Effects in Materials," NSWC/DL TR-3473, Naval Surface Weapons Center, Dahlgren Laboratory, Dahlgren, Virginia (July 1976).

7. R. A. Graham, "Piezoelectric Current from Shunted and Shorted Guard Ring Quartz Gauges," Journal of Applied Physics, Vol. 46, p. 190 (1975).

8. D. E. Munson and R. P. May, "Dynamically Determined High-Pressure Compressibilities of Three Epoxy Resin Systems," Journal of Applied Physics, Vol. 43, p. 962 (1972).

9. J. W. Nunziato and K. W. Schuler, "Evolution of Steady Shock Waves in Polymethyl Methacrylate," Journal of Applied Physics, Vol. 44, p. 4774 (1973).

DISTRIBUTION

Defense Documentation Center
Cameron Station
Alexandria, Virginia 21314 (12)

Defense Printing Service
Washington Navy Yard
Washington, D.C. 20374

Library of Congress
Washington, D.C. 20540
Attn: Gift and Exchange Division (4)

Commander
Naval Sea Systems Command
Washington, D.C. 20360
Attn: SEA-0333 W. W. Blaine
0333 R. A. Bailey
035 G. N. Sorkin
9921C L. H. Hawver

Commander
Naval Air Systems Command
Washington, D.C. 20360
Attn: AIR-310B J. W. Willis
320A T. F. Kearns

Office of Naval Research
Department of the Navy
Washington, D.C. 20360
Attn: ONR-420 T. G. Berlincourt
465 E. I. Salkovitz

Commander
Naval Research Laboratory
Washington, D.C. 20375
Attn: 6434 E. Skelton
7908 W. Atkins

Commander
Naval Weapons Center
China Lake, California 93555
Attn: J. Pearson
M. E. Backman
S. A. Finnegan

Superintendent
U. S. Naval Academy
Annapolis, Maryland 21402
Attn: Prof. J. Fontanella

Director
Army Ballistics Research Laboratories
Terminal Ballistics Laboratory
Aberdeen Proving Ground, Maryland 20015
Attn: G. E. Hauver
W. S. deRosset

Commander
Army Materials and Mechanics Research Center
Watertown, Massachusetts 92172
Attn: D. T. Dandekar
J. F. Mescall
P. V. Riffin

Commander
Army Picatinny Arsenal
Dover, New Jersey 07801
Attn: F. J. Owens
C. deFranco

Commander
Harry Diamond Laboratory
Washington, D.C. 20438
Attn: P. S. Brody

Los Alamos Scientific Laboratory
Los Alamos, New Mexico 87544
Attn: J. Wackerle
J. Morgan
J. M. Holt, Jr.
R. Morales
Technical Library (2)

Sandia Laboratories
Albuquerque, New Mexico 87115
Attn: B. M. Butcher
R. A. Graham
O. E. Jones
P. C. Lysne
R. R. Boade
D. E. Munson

Lawrence Livermore Laboratory
University of California 94550
Attn: D. L. Banner
W. H. Gust

Shock Dynamics Laboratory
Washington, State University
Pullman, Washington 99163
Attn: Prof. G. E. Duvall
Prof. G. R. Fowles

National Bureau of Standards
Washington, D. C. 20234
Attn: R. A. MacDonald
D. H. Tsai

Seismological Laboratory
California Institute of Technology
Pasadena, California 91125
Attn: Prof. T. J. Ahrens

Stanford Research Institute
Poulter Laboratory
333 Ravenswood Avenue
Menlo Park, California 94025
Attn: D. Curran
L. Seaman
D. Shockey

Local:

CC
CD
DC
DD
DF-12
DF-12 (Berger)
DG-10
DG-13
DG-20
DG-30
DG-33
DG-33 (Thompson)
DG-34
DG-40

DISTRIBUTION (Continued)

DG-50	
DG-52	
DG-52 (Mock)	(2)
DG-52 (Holt)	(2)
DG-52 (Wishard)	
DG-53	
DG-53 (Wenborne)	
DG-55	
DX-21	(2)
DX-222	(6)
DX-40	
DX-43 (Aids)	
WA-40	
WP	
WR-02	
WR-04	
WR-10	
WR-10 (Jacobs)	
WR-11 (Kamlet)	
WR-13	
WR-13 (Forbes)	
WR-13 (Erkman)	
WR-13 (Coleburn)	
WR-30	
WR-303	
WR-32	
WR-32 (Wang)	
WR-34	
WX-21	(2)